



HAL
open science

Microbe-induced coordination of plant iron-sulfur metabolism enhances high light stress tolerance of *Arabidopsis*

Kirti Shekhawat, Alaguraj Veluchamy, Anam Fatima, Gabriel X García-Ramírez, Jean-Philippe Reichheld, Olga Artyukh, Katja Fröhlich, Alexander Polussa, Sabiha Parween, Arun Prasanna Nagarajan, et al.

► To cite this version:

Kirti Shekhawat, Alaguraj Veluchamy, Anam Fatima, Gabriel X García-Ramírez, Jean-Philippe Reichheld, et al.. Microbe-induced coordination of plant iron-sulfur metabolism enhances high light stress tolerance of *Arabidopsis*. *Plant Communications*, 2024, pp.101012. 10.1016/j.xplc.2024.101012 . hal-04632797

HAL Id: hal-04632797

<https://hal.science/hal-04632797>

Submitted on 2 Jul 2024

HAL is a multi-disciplinary open access archive for the deposit and dissemination of scientific research documents, whether they are published or not. The documents may come from teaching and research institutions in France or abroad, or from public or private research centers.

L'archive ouverte pluridisciplinaire **HAL**, est destinée au dépôt et à la diffusion de documents scientifiques de niveau recherche, publiés ou non, émanant des établissements d'enseignement et de recherche français ou étrangers, des laboratoires publics ou privés.

Journal Pre-proof

Microbe-induced coordination of plant iron-sulfur metabolism enhances high light stress tolerance of *Arabidopsis*

Kirti Shekhawat, Alaguraj Veluchamy, Anam Fatima, Gabriel X. García-Ramírez, Jean-Philippe Reichheld, Olga Artyukh, Katja Fröhlich, Alexander Polussa, Sabiha Parween, Arun Prasanna Nagarajan, Naganand Rayapuram, Heribert Hirt

PII: S2590-3462(24)00329-8

DOI: <https://doi.org/10.1016/j.xplc.2024.101012>

Reference: XPLC 101012

To appear in: *PLANT COMMUNICATIONS*

Received Date: 15 April 2024

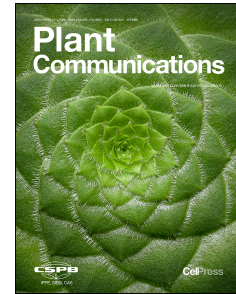
Revised Date: 11 June 2024

Accepted Date: 27 June 2024

Please cite this article as: Shekhawat, K., Veluchamy, A., Fatima, A., García-Ramírez, G.X., Reichheld, J.-P., Artyukh, O., Fröhlich, K., Polussa, A., Parween, S., Nagarajan, A.P., Rayapuram, N., Hirt, H., Microbe-induced coordination of plant iron-sulfur metabolism enhances high light stress tolerance of *Arabidopsis*, *PLANT COMMUNICATIONS* (2024), doi: <https://doi.org/10.1016/j.xplc.2024.101012>.

This is a PDF file of an article that has undergone enhancements after acceptance, such as the addition of a cover page and metadata, and formatting for readability, but it is not yet the definitive version of record. This version will undergo additional copyediting, typesetting and review before it is published in its final form, but we are providing this version to give early visibility of the article. Please note that, during the production process, errors may be discovered which could affect the content, and all legal disclaimers that apply to the journal pertain.

© 2024



1 **Microbe-induced coordination of plant iron-sulfur metabolism enhances high light stress**
2 **tolerance of Arabidopsis**

3 Kirti Shekhawat¹, Alaguraj Veluchamy², Anam Fatima¹, Gabriel X. García-Ramírez^{1,3}, Jean-
4 Philippe Reichheld^{4,5}, Olga Artyukh¹, Katja Fröhlich¹, Alexander Polussa⁶, Sabiha Parween¹, Arun
5 Prasanna Nagarajan¹, Naganand Rayapuram¹, Heribert Hirt^{1#}

6

7 ¹Biological and Environmental Sciences and Engineering Division, King Abdullah University of
8 Science and Technology (KAUST), 23955-6900 Thuwal, Saudi Arabia

9 ²Department of Computational Biology, St. Jude Children's Research Hospital, Danny Thomas
10 Place, Memphis 38105, TN, United States of America

11 ³ Max Planck Institute for Plant Breeding Research, 50829 Cologne, Germany

12 ⁴Laboratoire Génome et Développement des Plantes, Université Perpignan Via Domitia, F-
13 66860 Perpignan, France

14 ⁵Laboratoire Génome et Développement des Plantes, CNRS, F-66860 Perpignan, France

15 ⁶The Forest School, Yale School of the Environment, Yale University, New Haven, Connecticut,
16 USA

17 #Corresponding author: heribert.hirt@kaust.edu.sa

18 Running Title: SA187 mediates high light stress tolerance in *Arabidopsis thaliana*

19 **Summary:** Our research demonstrates that *Enterobacter* sp. SA187 enhances *Arabidopsis*
20 *thaliana* tolerance to high light stress by improving iron and sulfur metabolism through ethylene
21 signaling. SA187 promotes Fe-S cluster protein synthesis and strengthens the anti-oxidative
22 redox system, thereby maintaining photosynthesis and overall plant growth under high light
23 stress condition.

24 **Abstract**

25 High light stress in subtropical and tropical regions strongly limits agricultural production due to
26 photo-oxidative damage, decreased growth and yield. Here, we investigated whether beneficial
27 microbes can protect plants under high light stress. We found that *Enterobacter* sp. SA187
28 (SA187) supports *Arabidopsis thaliana* growth under high light stress by reducing the
29 accumulation of reactive oxygen species (ROS) and maintaining photosynthesis. When subjected
30 to high light stress, SA187 triggers dynamic changes in Arabidopsis gene expression related to
31 fortified iron metabolism and redox regulation thereby enhancing the plant anti-oxidative
32 glutathione/glutaredoxin redox system. Genetic analysis shows that SA187-enhanced iron and
33 sulfur metabolism are coordinated by ethylene signaling. In summary, beneficial microbes could
34 be an effective and inexpensive means for enhancing high light stress tolerance in plants.

35

36 **Key words:** high light stress, beneficial plant-microbe interaction, redox regulation,
37 glutaredoxins, ethylene signaling

38

39

40

41

42

43

44

45

46

47

48 Introduction

49 Light is a crucial factor for plants, serving as the primary energy source for photosynthesis and
50 playing a significant role in plant growth and development. However, excessive light can be
51 detrimental to plant growth by suppressing their photosynthetic capacity, leading to oxidative
52 damage to cellular organelles. There have been instances of excess daylight resulting in high light
53 stress for plants (D'Alessandro et al., 2020). For instance, in the northern hemisphere region (i.e.
54 Wisconsin, USA), the intensity can be upto $1400 \mu\text{mol}\cdot\text{m}^{-2}\cdot\text{s}^{-1}$ and is assumed to be constant
55 throughout the year (Handara et al., 2016). Under such high light conditions, excess electrons
56 cannot be passed to photosystem I (PS I) resulting in the accumulation of multiple reactive oxygen
57 species (ROS), including hydrogen peroxide (H_2O_2) and superoxide ($\text{O}_2^{\bullet-}$) (Apel and Hirt, 2004). In
58 such circumstances, rapid plant response mechanisms like non-photochemical energy quenching
59 (NPQ) dissipate excess energy as heat (Goss and Lepetit, 2015, Ruban, 2016; Schumann et al.,
60 2017; Shi et al., 2022). NPQ is a major factor in the rapid protection of Photosystem II (PSII)
61 reaction centers against photo-damage otherwise leading to photoinhibition of photosynthesis.
62 Plants also avoid damage to high light by changing the composition of the photosynthetic
63 apparatus, chloroplast and leaf avoidance movements or changes in leaf morphology (Walters,
64 2005, Schöttler and Tóth, 2014; Kasahara et al., 2002, Wada, 2013; Kim et al., 2005). To survive
65 and continue development under excess light conditions, plants activate the transcription of
66 genes encoding enzymes responsible for ROS scavenging (Rossel et al., 2002, Kleine et al., 2007,
67 Jung et al., 2013). To compensate ROS stress, plants also enhance glutathione production to
68 manage oxidative stress. Glutathione is the most abundant low-molecular-weight thiol in cells
69 and is a redox buffer that keeps the intracellular environment in a reduced state (García-Quirós
70 et al., 2019). Glutathione/Glutaredoxins are involved in the regeneration of enzymes involved in
71 peroxide and methionine sulfoxide reduction, constituting an important cellular system to
72 maintain redox homeostasis (Grant, 2001). Recently, it has been shown that glutaredoxins (GRXs)
73 can be engineered to attain enhanced oxidative stress tolerance in plants under abiotic stresses
74 such as temperature and light stress (Martins et al., 2020, Hendrix et al., 2023, Dard et al., 2023;
75 Knuesting et al., 2015; Rey et al., 2017; Cheng et al., 2011).

76 Although plants try to combat excess light conditions, they are not always successful in doing so,
77 resulting in irreversible cellular damage or cell death. In this context, studies have demonstrated
78 the effectiveness of plant growth-promoting bacteria (PGPB) in promoting plant growth under
79 abiotic stresses such as heat and iron (Harbort et al., 2020; Shekhawat et al., 2022). In this work,
80 we show that beneficial endophytic *Enterobacter* sp. SA187 isolated from root nodules of the
81 *Indigofera argentea* can enhance *A. thaliana* high light stress tolerance by coordinated iron and
82 sulfur acquisition, thereby strengthening the plant anti-oxidative system. We also show that the
83 beneficial effect of SA187 on high light stress is dependent on the plant ethylene signaling
84 pathway to reprogram the plant transcriptome for enhancing plant high light stress tolerance.
85 Overall, we propose that microbes that live in association with plants could be an effective system
86 for enhancing high light stress tolerance in crops.

87 **Results:**

88 **SA187 induces high light stress tolerance in *A. thaliana***

89 In order to assess the effect of SA187 on the growth of *A. thaliana* in high light stress, we
90 colonized *A. thaliana* plants with SA187 and exposed 5-day-old colonized and non-colonized
91 plants to normal light (NL) at $130 \mu\text{mol m}^{-2} \text{s}^{-1}$ and high light (HL) at $1050 \mu\text{mol m}^{-2} \text{s}^{-1}$ (Fig. 1A).
92 Compared to NL, exposure of non-colonized plants to HL led to chlorotic leaf damage (Fig. 1B)
93 and 129 % reduction of plant fresh weight (FW) (Fig. 1C). In contrast, SA187-colonized *A. thaliana*
94 plants were protected against HL chlorotic leaf damage and continued growth (Fig. 1B). To
95 investigate SA187-induced plant HL stress tolerance, we evaluated the FW of SA187-colonized-
96 HL treated (HL+187) to non-colonized-HL treated plants (HL). HL+187 exhibited 102% higher FW
97 levels than non-colonized plants (HL). This effect is HL stress specific, as under NL control
98 conditions, SA187-colonized (NL+187) and non-colonized plants (NL) displayed similar growth
99 (Fig. 1B) and FW (Fig. 1C). These data show that SA187 protects *A. thaliana* from HL stress and
100 enhances plant growth.

101 **SA187 improves plant growth under high light stress by increasing the Chlorophyll A and B** 102 **levels**

103 High light stress affects the photosynthetic machinery of plants and consequently chlorophyll
104 content. To check the performance of SA187-colonized plants under HL, we measured
105 chlorophyll A and B contents. As shown in Fig. 1D and E, compared to NL, HL stress significantly
106 reduced chlorophyll A and B levels by 134% and 82%, respectively. However, compared to non-
107 colonized HL plants, SA187-colonized-HL plants showed a significant increase in chlorophyll A and
108 B levels (Fig. 1D, E, 76% and 45%, respectively). The colonization of SA187 did not influence the
109 levels of chlorophyll A and B under control NL condition, indicating that SA187 mediates a
110 beneficial effect on *A. thaliana* only under HL stress (Fig. 1D, E).

111 **Dynamic transcriptome responses of *A. thaliana* seedlings to short-, mid-, and long-term high** 112 **light stress**

113 To investigate the underlying molecular events of HL stress on *A. thaliana*, we performed
114 transcriptome analysis of plants exposed to HL for 1h, 24h and 5d along with their respective
115 controls that were exposed to NL (S Fig. 1A-E). We used pairwise comparisons (e.g., 1h of NL
116 versus 1h of HL) to identify differentially expressed genes (DEGs) at each time point. The
117 expression profiles of all DEGs upon HL stress treatment fell into short-term (1h), mid-term (24h),
118 and long-term (5days) plant responses (Fig. 2). Considering DEGs with $P \leq 0.05$ and $FC \geq 2$ or ≤ -2 ,
119 a total of 1841 DEGs were observed at 1h, 2324 DEGs at 24h and 2,395 DEGs at 5day of HL stress,
120 respectively (Dataset 1).

121 To analyze transcriptional dynamics across different time points under high light (HL)
122 stress, we first organized the transcriptome data into 20 clusters before conducting gene
123 ontology (GO) enrichment analysis (Fig. 2). The transcriptome analysis in *A. thaliana* under HL
124 stress unveiled nuanced temporal responses, revealing distinct molecular events during various
125 phases of stress exposure. In the short term (1h), we identified a specific set of 524 genes (cluster
126 2) that were exclusively up-regulated. These genes were enriched in responses to abiotic stimuli,
127 cell redox homeostasis, and various stressors like HL intensity, oxidative stress, and heat stress.
128 This immediate response indicated the activation of stress-related pathways to cope with the
129 initial impact of HL. At 1h and 24h, we observed a distinct upregulated cluster of 244 induced
130 genes (cluster 4), which showed enrichment in responses to karrikin, water deprivation, abscisic
131 acid, light stimulus, and acidic chemicals. Interestingly, a cluster of 564 genes (cluster 5) was

132 gradually upregulated across all three time points (1h, 24h, and 5 days). Enrichment terms for
133 cluster 5 included autophagy, response to hypoxia, oxygen-containing compounds, and
134 programmed cell death, suggesting a sustained and coordinated cellular response correlating
135 with the observed HL-induced plant growth arrest over time. The 24h-HL response was notable
136 for a cluster of 658 upregulated genes (cluster 10) enriched in categories like sulfur metabolism,
137 anthocyanin and secondary metabolite biosynthesis, and redox processes. This behavior points
138 to an active adaptive plant response to counteract the stress conditions and maintain cellular
139 homeostasis. Clusters 18 and 19 highlighted genes specifically up-regulated after 5 days of
140 exposure, mainly involved in autophagy, hypoxia, and cell death.

141 We conducted an additional analysis focusing on genes consistently up-regulated in
142 response to high light (HL) stress across all three HL treatments. A Venn diagram highlights 32
143 genes (S Fig. 2) that are consistently up-regulated in all HL treatments. These genes are enriched
144 for high light intensity responses and can be regarded as high light (HL) signature genes such as
145 *ELIP1*, *HSP23.5*, *ROF2*, *HSP17.6A*, *HSP70b*, *HSP90.1*, *HOP3* and *TIN1*. In contrast, 52 genes were
146 consistently downregulated across all high light (HL) treatments. Notably, this set includes genes
147 encoding components of the photosynthesis machinery, such as *PSBT* and *PSBF* (Datasheet 2). In
148 summary, our findings provide a deeper understanding of the plant's sophisticated adaption
149 dynamics and contribute to the broader comprehension of plant stress responses.

150

151 **SA187 dynamically reprograms *A. thaliana* transcription under high light**

152 We next compared the molecular response of non-colonized to SA187-colonized *A. thaliana*
153 plants after 24h and 5days of exposure to HL stress. At 24h, in comparison to NL non-colonized
154 plants, and considering a $FC \geq 1.6$ or ≤ -1.6 ($P \leq 0.05$), 454 genes were differentially expressed in
155 SA187-colonized plants under NL conditions (Dataset 3). In contrast, 471 DEGs were found in
156 SA187-colonized (HL + 187) compared to non-colonized plants (HL) (Dataset 3) at 24h of HL stress
157 exposure. Compared to non-colonized plants (HL), SA187-colonization of plants (HL+187)
158 resulted in 414 DEGs at day 5 of HL. By contrast, comparing non-colonized (NL) to SA187-
159 colonized plants at 5 days of exposure to normal light conditions (NL+187) showed only 82 DEGs
160 (Dataset 3).

161 Under both normal and high light conditions, SA187 induced the expression of 18 genes
162 at 24 hours. These genes are characteristic of typical bacterial response genes, including *PR1*,
163 *PR5*, *SARD1*, and *FRK1*. After 5 days of high light exposure, 15 genes are induced (S Fig. 3 A-B),
164 including *CYP71A12*, *CML46* and *WRKY46* (Datasheet 4). Notably, only three genes (*AED1*,
165 *AT5G42530* and *AT2G25510*) were consistently up-regulated across all treatments (NL, NL+187,
166 HL, HL+187), while no common down-regulated genes were identified in these treatments (S Fig.
167 3 C-D).

168 **SA187 reprograms *A. thaliana* transcriptome related to photosynthesis and oxidative stress in** 169 **high light stressed plants**

170 We used heat maps to better understand how SA187-colonized *A. thaliana* responds to high light
171 (HL) conditions. The maps revealed differential gene expression patterns at 24 hours in both
172 normal light (NL) and HL settings (Fig. 3A). The DEGs identified at this 24-hour time point were
173 systematically categorized into 10 distinct clusters. Cluster 1, comprising 45 genes, emerged as
174 uniquely up-regulated due to SA187 colonization under NL. These genes exhibited a notable
175 enrichment in processes associated with lipid localization, transport, and macromolecule
176 localization. Clusters 2 and 3, encompassing 83 and 80 genes, respectively, exhibited a distinctive
177 downregulation in non-colonized plants under HL, a phenomenon observed to a lesser extent in
178 colonized plants subjected to HL (HL+187) (Fig. 3A). Genes within Cluster 2 were found to be
179 responsive to metal ion exposure, engaged in photosynthesis (involving multiple *LHCBS*, *PSAs*,
180 and *PSBs*), oxidative stress, and iron binding (*cICDH*, *FER1*, *FER3*, *FER4*, *MYB15*). In contrast,
181 Cluster 3 was characterized by enrichment in processes such as phosphorylation, response to
182 hormone stimulus, amino acid metabolism, and phosphate metabolism. Cluster 5, housing 159
183 genes, demonstrated specific up-regulation in colonized plants under HL conditions (HL+187)
184 (Fig. 3A). These genes were notably enriched in responses to bacterium, salicylic acid stimulus,
185 and redox metabolism, involving key elements such as peroxidases (*PRXs*), *ATBBE4*, *6*, *7*, *F6H1*,
186 *ARD1*, *FRO2*, *GA2OX8*, *HO3*, *PAD3*, and *SAG13*. Finally, Cluster 6, composed of 53 genes,
187 exclusively exhibited induction in non-colonized plants under HL, with no corresponding
188 induction observed in colonized HL-plants (HL+187) (Fig. 3A). These genes were enriched for
189 responses to water deprivation, osmotic stress, and abscisic acid.

190 In summary, the 24-hour transcriptome analysis revealed distinct gene expression profiles
191 related to photosynthesis (S Fig. 3E) and oxidative stress management in SA187-colonized *A.*
192 *thaliana*, highlighting a refined regulatory response compared to non-colonized plants under HL
193 conditions.

194 **Transcriptome data reveals that SA187 modulates the plant redox status via glutaredoxins**
195 **under long-term high light stress**

196 We employed a transcriptome heat map to assess *A. thaliana* response to prolonged HL stress
197 (Fig. 3B). Four clusters revealed distinct gene expression patterns (Fig. 3B). Cluster 4 consists of
198 94 genes, which showed higher transcript levels in non-colonized plants under HL treatment but
199 not in colonized plants (HL+187) (Fig. 3B). These genes showed enrichment for response to heat,
200 response to jasmonic acid and abscisic acid. Cluster 6 contains 120 genes that are down-regulated
201 in non-colonized plants under HL but less in SA187-colonized plants (HL+187) (Fig. 3B). These
202 genes showed enrichment for cell wall organization, lipid transport, photosynthesis, redox
203 metabolism and root development. Similarly, cluster 9 includes 67 genes that are down-regulated
204 in non-colonized plants (HL) but up-regulated by SA187 (HL+187) under HL conditions (Fig. 3B).
205 These genes exhibited GO-enrichment for photosynthesis, light harvesting (*CAB2*, *LHCB2.1*, *PSBE*,
206 *PSBH*, *PSBI*), redox homeostasis (*ROXY6*, 8, 9, 12, 14, 20), generation of precursor metabolites
207 and energy, disulfide and sulfur group redox metabolism. Cluster 10, likewise, exhibited
208 enrichment primarily in HL+187 and to a lesser extent in HL plants, specifically with terms such
209 as response to nitrogen compounds, oxygen-containing compounds, iron ion homeostasis,
210 ethylene and photosynthesis. The presence of SA187 elevated transcript levels of 22 genes
211 involved in the photosynthesis process. These genes include *PSAD-2*, *LHCB6*, *CAB2*, *PSAH2*,
212 *LHCB2.1*, *LHCB2.2*, *PSBX*, *LHCB4.3*, *PSAH-1*, *PSBTN*, *PSBQ-2*, *RBCS2B*, *RBCS1B*, *LHCB3*, *PSAN*, *PSBK*,
213 *PSBI*, *PSBZ*, *PSBJ*, *PSBH*, *PSAC*, and *NDHE* (S Fig. 3E). The transcriptome data of NL+187 and
214 HL+187-treated plants at 5 days indicated that SA187 colonization upholds gene expression
215 associated with photosynthesis and redox balance, orchestrated by glutaredoxins and the
216 biogenesis of Fe-S cluster proteins (S Fig. 4). The regulation of these genes suggests that SA187
217 positively influences the expression of key genes related to light harvesting, photosystem

218 components, electron transport, ultimately contributing to enhanced plant photosynthetic
219 activity.

220 **SA187 reprograms the plant proteome under long-term high light stress**

221 After 5 days of HL exposure, we performed LC-MS/MS protein analysis in SA187-colonized *A.*
222 *thaliana*. Using a fold change ≥ 1.6 and P value ≤ 0.05 , 40 proteins increased, and 34 decreased
223 (Datasheet 5). Up-regulated proteins showed enrichment in cytoplasm, organelle envelope,
224 plastid, and chloroplast. Interestingly, despite no overlap with the transcriptome, both analyses
225 highlighted enrichment in photosynthesis-related GO categories. Overall, 965 differentially
226 expressed proteins were identified without considering P values, with 408 up-regulated and 275
227 down-regulated in SA187-colonized-HL plants (Dataset 5). The GO analysis of the 408 up-
228 regulated proteins revealed GO terms such as: response to ROS, glycosyl compound and
229 tetrapyrrole metabolism, chloroplast, plastid thylakoid and iron-sulfur cluster binding (Datasheet
230 5). Although only 6 proteins showed an overlap between the up-regulated transcriptome and
231 proteome, similar GO categories, such as photosynthesis, response to reactive oxygen species,
232 and iron-sulfur cluster binding were obtained. Among the 6 common genes in the overlap
233 between proteome and transcriptome, two proteins of PSII (PSBH, PsbTn), showed enhanced
234 abundance in colonized plants (S Fig. 5). The protein analysis showed enrichment of proteins for
235 the iron-sulfur cluster binding category contained the following 6 proteins: Fe-S center of
236 cytochrome b6f complex PETC; Iron-Sulfur (Fe-S) cluster gene ARABIDOPSIS MITOCHONDRIAL
237 FERREDOXIN 1; FERREDOXIN C 2 (FdC2); CHLOROPHYLL A OXYGENASE (CAO); 2Fe-2S ferredoxin-
238 like superfamily protein; Methylthiotransferase (Dataset 3). These results support the hypothesis
239 that SA-187-colonized plants can grow under HL conditions by enhancing the resilience of the
240 photosystems via the continued biosynthesis of Fe-S proteins.

241 **Role of Fe in SA187-mediated rescue of plant growth under high light stress**

242 Iron is crucial for plant function, especially during the photosynthesis. Analysis of the
243 transcriptome data at 24 hours and 5 days of high light (HL) stress (S Fig. 6), revealed enrichment
244 for iron-related genes in colonized plants. These genes encompass various aspects of iron
245 metabolism, including those involved in iron starvation response (e.g., *AT5G40510*, *NPF2.5*,

246 *ATAGP22*, *RHS13*, *ZIP3*), in iron uptake and transport (e.g., *FRO2*, *FRO4*, *FRO6*, *IRT2*, *F6H1*), as
247 well as in iron storage (e.g., *FER1*, *FER3*, *FER4*). Therefore, we checked if SA187 could help *A.*
248 *thaliana* in Fe uptake under low iron conditions. As seen in Figure 4a-b, *A. thaliana* faced a 171%
249 reduction in FW under low iron conditions (low iron; 4mg FeNaEDTA/L) but showed a 131%
250 growth improvement with SA187-colonization (low iron+187). Control experiments with no iron
251 (0mg/L) revealed no growth for both SA187-colonized and non-colonized plants, indicating SA187
252 requires at least a minimal iron quantity for growth rescue (Fig. 4A-B). To further characterize the
253 role of iron in the SA187-induced HL tolerance, we used the *irt1-1* mutant that is deficient in iron
254 uptake. *irt1-1* plants showed a growth deficit and leaf chlorosis phenotype under HL stress. In
255 contrast to WT plants, the phenotype of *irt1-1* mutant plants could not be improved by
256 colonization of SA187 (Fig. 4C-D), indicating the important role of iron import in the SA187-
257 induced tolerance mechanism under HL stress. To eliminate the possible discrepancies in
258 bacterial colonization, we evaluated the effect of *irt1-1* mutant and HL stress on SA187
259 colonization. The results at 5 and 10-days of HL stress in Col-0, *irt1-1* mutants revealed no
260 significant differences in colony-forming unit (CFU) levels between wild type and mutants,
261 indicating that the mutants do not affect the overall colonization in *A. thaliana* under NL or HL
262 conditions (S Fig. 7). In low iron conditions (8 mg/L), plants exposed to HL stress (HL-Fe) exhibited
263 a 61% reduction in FW compared to iron-sufficient conditions (HL+Fe) (Fig. 4E). Conversely, under
264 low iron conditions, SA187-colonized plants (HL-Fe+187) outperformed non-colonized plants (HL-
265 Fe) (Fig. 4E). Increasing FeNaEDTA levels in the medium under HL stress (HL++Fe) had significant
266 growth benefits, akin to SA187 colonization (Fig. 4F). Iron addition increased fresh weight by 80%
267 (HL++Fe) compared to non-treated HL plants (HL+Fe). Notably, the combined treatment of SA187
268 and increased FeNaEDTA (HL+Fe+187) showed the highest fresh weight increase at 110% under
269 HL stress (Fig. 4F). Iron levels in shoot and root were assessed in non-colonized and SA187-
270 colonized plants under NL and HL conditions (Fig. 4G, H). Under NL conditions, SA187 inoculation
271 did not impact iron concentrations. However, under HL conditions, SA187 increased iron levels
272 in the shoot and root by 35% and 33%, respectively (Fig. 4H).

273 **Sulfur plays an important role in SA187 mediated high light stress tolerance**

274 Sulfur is essential for photosynthesis due to its roles in protein synthesis, enzyme activity,
275 chlorophyll production, and redox regulation. High light (HL) stress can damage Fe-S proteins,
276 mainly in PSI and ferredoxin. Our transcriptome data revealed DEG enrichment of sulfur
277 compound and amino acid metabolic processes after 24 hours and 5 days of HL exposure in
278 colonized plants, including *BGLU34*, *BGLU35*, *BCAT6*, *CYP81F2*, *IGMT1*, *NAC042*, and *WRKY70* (S
279 Fig. 8). Additionally, genes containing Fe-S cluster proteins (*ABCI*, *NEET*, *PSAC*) were upregulated
280 in HL+187 conditions. Increased sulfate concentrations in the medium have also been reported
281 to help plants to withstand various abiotic stresses such as salt stress. Therefore, we compared
282 the growth of plants under HL stress with increased $MgSO_4$ levels in the medium (S Fig. 9). Under
283 HL stress, the addition of sulfate (HL+S) showed significant beneficial effects on plant growth
284 similar to colonization by SA187 (S Fig. 9). The addition of sulfate increased FW by 90% (HL+S),
285 when compared to non-treated HL plants (Mock+HL). Examining *sultr1;2*, *sir1-1*, and *IsuC* mutant
286 plants highlighted the key role of the plant sulfur metabolism in HL stress tolerance. Importantly,
287 SA187 showed the ability to enhance the growth of these mutants under HL stress, highlighting
288 its potential as a stress ameliorator (S Fig. 9).

289 **SA187 reduces ROS levels and affects the cytoplasmic redox state under high light stress**

290 High light stress induces ROS production in the chloroplast, and one of the major drastic effects
291 of ROS is the inhibition of the photosynthetic machinery. To test the possibility that SA187
292 protects *A. thaliana* from excessive ROS levels, we examined superoxide levels in SA187-
293 colonized and non-colonized plants grown under control, NL and HL stress conditions. Nitroblue
294 tetrazolium staining showed that SA187 colonization did not enhance superoxide radical levels
295 under normal light conditions (Fig. 5A). However, under HL conditions, SA187-colonized plants
296 (HL+187) showed reduced superoxide levels when compared to non-colonized HL plants (Fig. 5A).
297 Since HL-induced ROS can disturb the redox status of cells, we compared the redox status of
298 SA187 colonized to non-colonized plants under HL stress. We used a cytosolic GRX1/ro-GFP2
299 tagged reporter line to monitor the *A. thaliana* response to HL-imposed redox changes in SA187-
300 colonized and non-colonized plantlets. The ro-GFP2 fluorescence was collected at 505-530 nm
301 after excitation with either 405 nm or 488 nm. The ratio of images was calculated as 405/488 nm
302 fluorescence. When evaluating the ro-GFP2 redox ratio, specifically focusing on leaf cytosol (Fig.

303 5C), we noted gradual partial oxidation after 24 hours, 5 days, and 10 days of high light (HL). In
304 contrast, there was a progressive reduction observed in SA187-colonized plants under HL
305 (HL+187). The redox ratios were significantly higher in non-colonized plants when compared to
306 SA187-colonized plants at 5 and 10 days of HL stress (Fig. 5B-C). After 10 days of HL, non-
307 colonized plants showed a 405/488 ratio of 0.72 (partial oxidation), while SA187-colonized plants
308 showed 0.45 (fully reduced), indicating that SA187-colonized plants have a fortified redox
309 balance under HL stress. As a control, we used 10mM DTT and 100mM H₂O₂ to fully reduce or
310 oxidize the ro-GFP2 (Fig. 5B, D). The ro-GFP2 is monitoring the glutathione (GSH) redox
311 homeostasis. Since the synthesis of glutathione is tightly linked to ROS protection, one possible
312 explanation for these results could be that SA187-colonized plants have higher redox capacity
313 due to improved GSH synthesis. To confirm this, we used *cad2-1* mutant, characterized by a
314 deficiency in gamma-glutamylcysteine synthetase—a pivotal enzyme in glutathione biosynthesis.
315 *cad2-1* mutant plants exhibited retarded growth phenotypes under normal conditions due to
316 reduced glutathione synthesis. However, the growth of *cad2-1* mutants is ameliorated in the
317 presence of SA187. When subjected to HL stress, non-colonized plants exhibit significant growth
318 inhibition in contrast to SA187-colonized plants (Fig. 5E). These findings emphasize the role of
319 SA187 in maintaining glutathione levels, providing a protective effect against damage induced by
320 triggered by HL stress.

321 **SA187 improves the plant thiol redox balance under high light conditions**

322 The generation of ROS induced by high light leads to protein inactivation through the oxidation
323 of thiol groups. To assess this, we measured the thiol content in SA187-colonized and non-
324 colonized plants under NL and HL stress conditions at days 5 and 10. At day 5, HL treatment for
325 5 days resulted in a 9-fold reduction in total protein thiol compared to NL conditions (S Fig. 10A).
326 Conversely, SA187-colonized plants exhibited a slight increase in protein thiol content under both
327 NL and HL conditions (S Fig. 10A). Moreover, plants colonized by SA187 exhibited increased levels
328 of non-protein thiol content under high light (HL) stress, potentially attributable to elevated
329 glutathione (S Fig. 10B), contributing to an overall increase in total cellular thiol compared to non-
330 colonized plants (S Fig. 10C). Notably, these findings provide additional support for the SA187-
331 mediated growth rescue of *cad2-1* mutant plants. After 10 days of HL stress, SA187-colonized

332 plants demonstrated a reduction in non-protein thiol content and a 92% increase in protein thiol
333 content compared to non-colonized HL-plants (S Fig. 11). These findings suggest that the
334 presence of SA187 alleviates protein thiol oxidation in HL-treated plants, but also induces non-
335 protein thiol level in the context of HL.

336 **Plant glutaredoxins play an important role in SA187-mediated high light stress tolerance**

337 Glutaredoxins are key proteins to protect cells from oxidative stress and are known to be involved
338 in the biogenesis of Fe-S clusters as well as redox reactions (Lill et al., 2008; Rouhier et al., 2008,
339 2010). Since our transcriptome data showed enrichment for the transcript of different
340 glutaredoxins and disulfide oxidoreductase activity, we examined the role of the cytosolic iron-
341 sulfur cluster glutaredoxin *GRXS17* in SA187-Mediated high light stress tolerance. *grxs17*-
342 colonized and non-colonized mutant plants were subjected to NL and HL conditions. As shown in
343 S Fig. 10D the *grxs17* mutant plants suffered significantly under HL stress compared to wild-type
344 plants, exhibiting a reduction of 70% FW (S Fig. 10D, E). Unlike wild-type Arabidopsis which were
345 protected from high light stress (112% higher FW compared to non-colonized HL treated plants),
346 SA187 colonized *grxs17* mutant plants were compromised in the SA187 beneficial effect under
347 HL stress (S Fig. 10D, E). These results indicate the importance of glutaredoxins in SA187-
348 mediated HL stress tolerance mechanism in plants.

349 **Ethylene is a key regulator of SA187-mediated high light stress tolerance**

350 The transcriptome analysis of plants at 5 days of high light (HL) treatment revealed a significant
351 GO term enrichment for ethylene in SA187-colonized plants compared to the non-colonized
352 counterpart. This enrichment encompassed various aspects of ethylene biosynthesis and
353 signaling, involving genes such as *ACS4*, *ACS6*, *ACS5*, *ETO2*, *ERF2*, *ERF13*, *ERF15*, *TN7*, *AT1G28370*,
354 *AT4G29780*, *ATAVT6B*, and *WRKY40* (Fig. 3B) (S Fig. 8). Moreover, previous studies showed that
355 ethylene is a key regulator in SA187-mediated plant growth under heat and salt stress
356 (Shekhawat et al., 2021; de Zélicourt et al., 2018). To test whether ethylene also plays a role
357 in SA187-induced HL stress tolerance, we analyzed the ethylene-insensitive *ein3-1* mutant under
358 NL and HL conditions. As shown in Fig. 6A, unlike wild type, *ein3-1* mutants were compromised
359 in SA187-mediated HL stress resistance, indicating that EIN3 is involved in SA187-mediated HL

360 stress tolerance. We further confirm these results in ethylene-insensitive *ein2-1* mutant plants (S
361 Fig. 12A, B). Iron uptake is regulated by ethylene (Lucena et al., 2015), therefore, we also analyzed
362 whether SA187 is compromised in ethylene mutants under low iron conditions. Unlike in wild-
363 type plants, SA187 could not restore the phenotype of *ein3-1* mutants under low iron conditions
364 (Fig. 6B). These results indicate that the ethylene pathway is also involved in SA187-mediated
365 enhanced iron uptake under normal conditions of light intensity. To confirm that ethylene
366 signaling mediates plant HL stress tolerance by SA187, we performed qRT-PCR of *ein3-1* mutant
367 plants for *FRO2* and *LHCB* genes after 24 h and 5 days of HL treatment. SA187-colonized *ein3-1*
368 plants were compromised in inducing higher transcript levels of these genes under HL stress
369 when compared to wild-type plants, confirming EIN3-dependent induction of HL stress tolerance
370 by SA187 (Fig. 6C, F). We further confirmed our hypothesis by verifying the gene expression of
371 *IGMT1*, *BCAT6*, *LSU1*, *CYP17A12*, *HO3* and *FER4* genes (S Fig. 13). To eliminate the possible
372 discrepancies in bacterial colonization, we evaluated the effect of *ein2-1* mutant and high light
373 stress on SA187 colonization. The results at 5 and 10 days of HL stress in Col-0, *ein2-1* mutants
374 revealed no significant differences in CFU levels, indicating that the ethylene mutant does not
375 affect the overall colonization of *A. thaliana* by SA187 under NL or HL conditions (S Fig. 7).

376 Discussion

377 Light is vital for plant growth, serving as the main energy source. However, excess light absorption
378 can lead to increased production of ROS, causing photo-oxidative damage and inhibiting
379 photosynthesis. Our data confirm previous reports that plants respond to short-, mid- and long-
380 term HL stress by dynamic transcriptional changes (Huang et al., 2019). Transcriptome analysis
381 uncovered the relative dynamics of transcriptional changes. Complex transcriptional responses
382 occur in plants when exposed to different timescales of HL stress. The novelty of our work is that
383 microbes can assist plants in maintaining growth under such stress conditions (Fig. 1B-C).
384 Mitochondria and chloroplasts rely on abundant iron and sulfur for essential functions, such as
385 photosynthesis, respiration, DNA repair, and ribosome biogenesis, which are all facilitated by Fe-
386 S cluster-containing proteins (Rouhier et al., 2010). Our research unveils the mechanisms by
387 which SA187-mediated ethylene signaling orchestrates iron and sulfur metabolism, bolstering
388 Arabidopsis tolerance to HL stress. Under HL, plants accumulate reactive oxygen species (ROS),

389 which impair Fe-S cluster proteins vital for photosynthesis. Transcriptomic and phenotypic
390 analyses reveal that SA187 enhances plant uptake of Fe and S, supporting the synthesis of Fe-S
391 cluster proteins essential for photosynthesis machinery maintenance under stress. Moreover, we
392 find that SA187 colonization rescues plant growth under Fe-limiting conditions during HL stress.
393 Supplementation with Fe and S, similarly enhances plant resilience to HL, akin to SA187
394 colonization. SA187 promotes iron acquisition by upregulating root (*FRO2*, *FRO4*, *FRO6*, *IRT2*) and
395 chloroplast-associated (*FER1*, *FER3*, *FER4*, *ZIP3*, *HO3*) iron genes. The elevated transcripts of root-
396 associated genes could be attributed to the enhanced root formation observed in plants
397 colonized by SA187 under HL stress conditions. While previous studies have highlighted the
398 beneficial role of microbes in aiding plants under iron-limiting conditions (Zamioudis et al., 2014;
399 Verbon et al., 2017; Harbort et al., 2020; Montejano-Ramírez et al., 2023), our study brings forth
400 a novel aspect by revealing that microbes can also confer protection to plants under high light
401 stress, which consequently induces iron limitation. This finding highlights the complex role of
402 microbial colonization in plant resilience, particularly in challenging environmental conditions
403 such as high light stress. Proteomic analysis verified increased Fe-S cluster and photosystem
404 protein levels in SA187-colonized plants upon 5 days of HL exposure. Additionally, MgSO₄
405 supplementation augmented plant performance under HL stress. Analysis of *sultr1;2*, *sir1-1*, and
406 *IsuC* mutant plants underscores the pivotal role of the plant sulfur metabolism in HL stress
407 tolerance. Remarkably, SA187 enhances the growth of these mutants under HL stress,
408 highlighting its potential as a stress ameliorator. Photosynthetic organisms have evolved a variety
409 of direct and indirect mechanisms for HL stress management including ROS
410 production/scavenging, stomatal regulation, and systemic signaling (Mignolet-Spruyt et al., 2016;
411 Huang et al., 2019; Shi et al., 2022; Barczak-Brzyżek et al., 2022). In this context, our data revealed
412 that SA187 induces the expression of several peroxidases such as *PRX*, *31*, *37*, *69* and *71* at 24h;
413 while *PRX01*, *2*, *FSD1* and other peroxidases accumulate in long-term HL. Higher expression of
414 these peroxidases helps plants to scavenge ROS and maintain photosynthetic activity (Lu et al.,
415 2017; Fryer et al., 2003; Melicher et al., 2022). In addition, the antioxidative process relies on
416 glutathione, which facilitates the reduction of disulfide-containing proteins by glutaredoxins
417 (Holmgren, 1989; Gleason and Holmgren, 1988). Glutaredoxins undergo oxidation by substrates

418 and are non-enzymatically reduced by glutathione. This glutathione/glutaredoxin system plays a
419 crucial role in maintaining redox homeostasis (Grant, 2001). Multiple pieces of evidence suggest
420 that glutathione and glutaredoxins play a role in responding to oxidative stress by rejuvenating
421 enzymes involved in disulfide protein reduction. Moreover, glutaredoxins are versatile proteins
422 involved in various functions, including Fe-S cluster biogenesis, encompassing iron and sulfur
423 acquisition, cluster assembly, transfer, and maintenance. Our data from HL stress experiments
424 on both colonized and non-colonized plants demonstrates that the presence of SA187 boosts the
425 expression of a cluster of at least 8 glutaredoxin genes after 5 days of exposure to HL. This implies
426 that SA187 prompts the elevation of the GRX/glutathione system to reinforce the redox
427 equilibrium. This hypothesis is supported by the loss of the beneficial effect of SA187 in *grxs17*
428 mutant plants under HL stress. GRXs can be engineered to enhance oxidative stress tolerance in
429 plants and to investigate redox-controlled processes in temperature stress tolerance (Kapoor et
430 al., 2015; Martins et al., 2020; Kumar et al., 2021). AtGRXS17 plays a role in anti-oxidative stress,
431 tolerance to iron deficiency and thermotolerance in both yeast and plants (Wu et al., 2012; Yu et
432 al., 2017; Cheng et al., 2020) and transgenic expression of fern *Pteris vittata* glutaredoxin *PvGrx5*
433 in *A. thaliana* increases tolerance to high-temperature stress and reduces oxidative damage to
434 proteins (Sundaram and Rathinasabapathi, 2010). Proper performance of the GRXs/glutathione
435 system is involved in maintaining the thiol redox balance of the thiol proteins. We therefore also
436 checked the protein and non-protein thiol content of SA187-colonized and non-colonized plants
437 under NL and HL conditions. The protein thiol contents decreased in HL treatment, but to a lower
438 level in SA187-colonized plants. Moreover, the non-protein thiol content was higher in SA187
439 colonized compared to non-colonized plants under HL. These data show that SA187 maintains
440 the protein thiol status via an improved anti-oxidant system. Oxidative stress is expected to
441 increase the sulfur flux to sulfur reduction for the production of the redox buffer GSH/GSSG. We
442 suggest that SA187 helps to improve both sulfur and iron homeostasis to maintain the redox
443 balance and thereby reduce HL-induced oxidative damage in *A. thaliana* (Fig. 7).

444 In our study, we discovered that ethylene is crucial for SA187-induced HL stress tolerance in
445 plants. Our findings highlight the compromised HL tolerance in *ein3-1* mutant plants, underlining
446 the importance of the ethylene pathway and EIN3 transcription factor. Moreover, ethylene

447 signaling is vital for regulating iron uptake mechanisms, as shown by the poor growth of *ein3-1*
448 mutants under iron-limiting conditions. Interestingly, SA187-colonized *ein3-1* plants displayed
449 compromised growth under low iron conditions, unlike their wild-type counterparts. This
450 observation suggests that SA187-induced ethylene signaling is vital for maintaining an adequate
451 iron supply during HL stress. Previous research has also shown that, under iron deficiency
452 conditions, EIN3 up-regulates FIT1, consequently influencing the expression of *IRT1* and *FRO2*
453 genes (Yang et al., 2022). The modified synthesis of phytohormones in plants by beneficial
454 microbes influences the plant responses to iron deficiency. Similarly, ethylene signaling in *A.*
455 *thaliana* plays a role in regulating the sulfur regulon, which encompasses a significant portion of
456 sulfur metabolic enzymes. This regulation influences sulfate uptake, contributing to the synthesis
457 of precursors for protein synthesis and antioxidants like glutathione for mitigating cellular ROS
458 levels. The diminished upregulation of iron and sulfur genes observed in SA187 colonized *ein3-1*
459 plants (Fig. 7; S Fig. 13) highlight the central role of ethylene in orchestrating plant responses to
460 iron and sulfur homeostasis under stress conditions, rationalizing why SA187-induced ethylene
461 signaling is crucial for sustaining iron and sulfur levels during HL stress. We further analyzed the
462 SA187 genome, revealing the presence of genes encoding enterobactin and aerobactin
463 siderophores (S Fig. 14A). The results on Chrome Azurol S (CAS) plates also demonstrated
464 siderophore production by SA187 (S Fig. 14B). Additionally, genes involved in iron metabolism
465 (*entB*, *YbdZ*, Enterobactin synthase components B and F, Ferric aerobactin receptor, and *FepD*)
466 (S Fig 15) were upregulated after 6 hours of growth on CAS plates compared to LB media, as well
467 as in colonized plants under high light (HL) stress compared to normal light (NL) (specifically *entB*
468 and *YbdZ*) (S Fig. 15 B,D). These findings support the idea that SA187 utilizes its iron metabolism
469 to enhance plant growth under HL stress conditions.

470 In summary, our data support the notion that colonization with SA187 can shield plants
471 from extreme oxidative stress conditions such as HL stress. The findings highlight the nuanced
472 impact of microbial colonization on plant stress resilience, particularly in sustaining crucial
473 processes like photosynthesis and redox homeostasis. Protection against these stresses is
474 achieved through ethylene-dependent signaling that enhances iron and sulfur acquisition levels,

475 ultimately fortifying the antioxidative redox system. As a result, SA187 helps maintain
476 photosynthesis and overall plant growth under challenging HL stress conditions.

477 **Materials and Methods**

478 **Bacterial inoculum and media preparation**

479 The endophytic bacterial strain, *Enterobacter* sp. SA187 was isolated from root nodules of
480 *Indigofera argentea* collected from the Jizan region of Saudi Arabia (Andrés-Barrao et al., 2017).
481 Before performing the plant colonization experiments, the cryogenically maintained SA187 strain
482 was streaked out on LB agar media and incubated at 28°C for 24 h. A single colony was used for
483 further experiments. For bacterial seed plates, 50 ml of half-Murashige and Skoog medium (MS)
484 with 0.9% agar and a pH of 5.8 was mixed with 0.1 ml of fresh bacterial suspension with an OD
485 of 0.2 to obtain a final number of 10^5 CFU ml⁻¹. For control plates, 0.1 ml of liquid LB was mixed
486 with ½ MS media.

487 **Plant material and growth conditions for *A. thaliana***

488 *A. thaliana* wild-type Col-0 seeds and mutants (*irt1-1*, *ein3-1*, *cad2-1*, *sir1-1*) were obtained from
489 publicly available collections. While seeds of GRX1/ro-GFP2 and *grxs17* mutant lines were
490 obtained from Jean-Philippe Reichheld's lab. Seeds were surface-sterilized with 0.05% SDS,
491 followed by three times washing with absolute ethanol. The sterilized seeds were plated on ½
492 MS medium agar plates seeded with 10^5 CFU/ml SA187. Seeds were stratified at 4°C for 2 days
493 and then plates were transferred to growth chambers (Model CU36-L5, Percival Scientific, Perry,
494 IA, USA) for growth. For high light experiments, after 5 days, SA187-inoculated and non-
495 inoculated seedlings of near equal lengths were transferred to new ½ MS plates. For the high
496 light stress experiment, SA187 treated and non-treated control plants were transferred to 16h
497 high light intensity of $1050 \mu\text{mol m}^{-2} \text{s}^{-1}$ in Biochamber (Huang et al., 2019). For control
498 conditions, the colonized and non-colonized plants were transferred to a 16h normal light
499 condition of $130 \mu\text{mol m}^{-2} \text{s}^{-1}$. The light was measured by the Spectroradiometer SPR-03
500 (Luzchem). The temperature of the high light chamber was maintained by cool airflow from the
501 bottom of the chamber to make sure the medium and leaf temperatures were kept at 22°C to
502 match the control growth condition. Samples were harvested at 1 h, 24 h and 5 days of high light
503 treatment. The control plants were kept in the $130 \mu\text{mol m}^{-2} \text{s}^{-1}$, 22°C chamber for collecting

504 control samples at each time point. Sterile conditions were maintained throughout the
505 experiment by ensuring the plates were securely sealed with surgical tape, effectively preventing
506 any external contamination from compromising the results.

507 **Chlorophyll measurements**

508 Chlorophyll a and b were extracted from 50 mg frozen shoot samples with 80% acetone (Arnon,
509 1949; Sims and Gamon (2002). After centrifugation, supernatant was used to measure OD at 537,
510 647, 645, and 663 nm. Following formula was used to calculate Chl a/b: Chl a ($\mu\text{mol ml}^{-1}$) =
511 $0.01373 A_{663} - 0.000897 A_{537} - 0.003046 A_{647}$; Chl b ($\mu\text{mol ml}^{-1}$) = $0.02405 A_{647} - 0.004305$
512 $A_{537} - 0.005507 A_{663}$.

513 **RNA extraction, reverse transcription, and qRT-PCR**

514 For RNA-seq analysis, total plant RNA was extracted from colonized and non-colonized plants
515 exposed to normal light (NL) and high light stress conditions using the Nucleospin RNA plant kit
516 (Macherey-Nagel), including DNaseI treatment, according to the following manufacturer's
517 recommendations. For qPCR analysis, the total RNA was reverse-transcribed using a using
518 Superscript III (Invitrogen): 1 μg of total RNA and oligo-dT as primer were used for the cDNA
519 synthesis according to the manufacturer's protocol. For *A. thaliana* gene expression analyses,
520 tubulin was used as a reference gene. All reactions were done in a CFX96 Touch Real-Time PCR
521 Detection System (Bio-Rad) as follows: 50°C for 2 min, 95°C for 10 min; 40 \times (95°C for 10 s and
522 60°C for 40 s). All reactions were performed in three biological replicates, and each reaction as a
523 technical triplicate. The reference genes used in this analysis was ACTIN2 (At3g18780) (33), gene
524 expression were normalized against reference gene.

525 **Bioinformatics analysis of RNA-seq data**

526 Concentration and purity of RNA were determined by spectrophotometry and integrity was
527 confirmed using an Agilent 2100 Bioanalyzer with an RNA 6000 Nano Assay (Agilent Technologies,
528 Palo Alto, CA, USA). The RNA samples with RNA integrity number (RIN) more than 8, and 280:260
529 ratios more than 2 were further used for the RNA-sequencing purpose. We performed mRNA
530 libraries of total plant RNA using Illumina mRNA Library Prep kit. Libraries were sequenced using
531 the Illumina HiSeq 4000 platform. We checked the quality of the sequenced reads using FASTQC
532 (Andrews, 2010). The low-quality reads or base pairs and the adaptors were trimmed using

533 Trimmomatic V0.36 (Bolger et al., 2014). The trimmed reads were then aligned using TopHat
534 v2.2.1 to the TAIR10 and SA187 genome combined (Trapnell et al., 2009; Trapnell et al., 2012;
535 Kim et al., 2013). Reads per million bases and differential expression between two conditions
536 were calculated using Cufflinks v2.2.0 (Trapnell et al., 2009). To identify differentially expressed
537 genes, specific parameters (P-value ≤ 0.05 ; statistical correction: Benjamini–Hochberg; FDR \leq
538 0.05) in cuffdiff were used. Post-processing and visualization of differential expression were done
539 using cummeRbund v2.0.0. A cut-off of 2-fold change and P-value less than 0.05 were set to
540 identify the up- and down-regulated genes between NL and HL conditions; while a cut-off of 1.6-
541 fold change and P-value ≤ 0.05 were set to identify the up- and down-regulated genes between
542 HL and HL+187 treatments. AgriGO (Tian et al., 2017) was used to find the corresponding GO
543 terms (FDR ≤ 0.05) and the functions of the respective genes. Venny (Oliveros, 2007–2015) was
544 used to identify common or unique. The cluster analysis was conducted using MeV
545 (MultiExperiment Viewer) software, which allows for comprehensive data visualization and
546 analysis. This software enabled us to organize and interpret the complex datasets, providing
547 insights into the relationships and patterns within the gene expression data.

548 **Quantification of SA187-colonization**

549 Seedlings were initially cultivated on $\frac{1}{2}$ MS agar plates inoculated with SA187, and 5-day-old
550 seedlings were subsequently transferred to fresh $\frac{1}{2}$ MS plates. On the 6th day, the plants were
551 subjected to NL and HL exposure for 5 days and 10 days, to conduct colony-forming unit (CFU)
552 analysis. The plants were homogenized by grinding. The resulting sample was then suspended in
553 1 milliliter of an extraction buffer containing 10 mM $MgCl_2$ and 0.01% Silwet L-77. Subsequently,
554 serial dilutions were carried out, and the diluted samples were plated on LB agar plates. After an
555 overnight incubation at 28°C, the CFUs were enumerated. The calculated CFU values were
556 normalized based on the weight of plant material (per milligram).

557 **Protein extraction and sample preparation**

558 In this experiment, *A. thaliana* WT plants were grown under high and normal light conditions for
559 five days. The plants were harvested, frozen, and powdered. The proteins were extracted using
560 a lysis buffer and then purified through a series of steps, including methanol/chloroform
561 precipitation. The resulting proteins were quantified and digested into peptides. After desalting,

562 the samples were prepared for mass spectrometry analysis using Data-Independent Acquisition
563 (DIA) to study the plant's protein content. This workflow allows for a detailed analysis of protein
564 changes in response to different light conditions.

565 **DIA-MS analysis**

566 The peptide samples were subjected to DIA-MS analysis using an Orbitrap Fusion Lumos mass
567 spectrometer (Thermo Scientific) coupled with an UltiMate 3000 UHPLC (Thermo Scientific),
568 following the methodology outlined in Zhang et al. (2019). In brief, Peptide samples (1.5 μg)
569 underwent DIA-MS analysis using a Thermo Scientific Orbitrap Fusion Lumos mass spectrometer
570 coupled with UltiMate 3000 UHPLC. The peptides were desalted, separated over a 130-minute
571 gradient, and analyzed in triplicate injections. DIA-MS data were collected for three precursor
572 mass ranges (400–650; 650–900; 900–1,200 m/z) with isolation windows of 6–8 Da. HCD collision
573 energy was set at 30%, and MS parameters included resolutions of 60,000 for MS1 and 30,000
574 for MS/MS. The protocol utilized EASY-IC for internal mass calibration, and maximum ion
575 accumulation time was 100 ms with a target value of $1e6$.

576 **DIA-MS data analysis**

577 DIA-MS data was analyzed using Spectronaut software (version 14) with an in-house generated
578 *A. thaliana* spectral library. Default Biognosys settings were used for identification, and a paired
579 Student's t-test was performed to find differentially expressed proteins between control and
580 mutant samples. Multiple testing correction was applied to control the False Discovery Rate
581 (FDR). Proteins with a fold-change greater than 1.5 were considered differentially expressed. GO
582 enrichment analysis was conducted using AgriGO (V2) and Revigo to reduce redundant GO terms.

583 **Quantification of total thiol, non-protein thiols and protein thiol**

584 TT and PT contents were determined according to Sedlak and Lindsay 1968. *A. thaliana* seedlings
585 weighing 50 mg were homogenized in 1000 μL of 0.2M Tris-HCl (pH 7.4) and centrifuged at 10
586 000 $\times g$ for 20 min at 4°C. The supernatant was used to assay TT and NPT. To determine the TT,
587 50 μL of supernatant was mixed with 150 μL of 0.2mM Tris-HCl (pH 8.2), 10 μL of 0.01 M DTNB
588 and 790 μL of absolute methanol. The yellow color that developed was measured after 15 min at
589 415 nm against a blank vial containing 50 μL of distilled water instead of supernatant. Total
590 sulfhydryl groups were calculated based on an extinction coefficient of 13,600 and expressed as

591 μmol per g fresh weight. To determine of NPT content, 500 μL ml of supernatant was mixed with
592 400 μL of distilled water and 100 μL of 50% TCA. After 15 min. the mixture was centrifuged at 10
593 000 x g for 15 min. In 200 μL of deproteinized supernatant, NPT concentration was measured like
594 that for TT. PT was calculated by subtracting the NPT content from the TT content.

595 **Confocal microscopy of ro-GFP2**

596 SA187-colonized and non-colonized high light stress treated GRX1/ro-GFP2 seedlings were
597 imaged using an inverted Zeiss LSM 880 confocal microscope equipped with Plan-Apochromat
598 10x/0.45, Plan-Apochromat 20x/0.8, Plan-Apochromat 40x/1.4 Oil objectives, and the ZEN 2010
599 software (Zeiss). The excitation of HL-treated colonized and non-colonized ro-GFP2 was
600 performed at 488 nm and 405 nm, and a bandpass (BP 490-555 nm) emission filter was used to
601 collect the ro-GFP2 signal. Picture analysis and quantifications of the ro-GFP2 redox ratios
602 (405/488) were performed using the Redox Ratio Imaging software (Fricker, 2016).

603

604 **CAS assay for siderophores detection**

605 The production of siderophores was determined using the Blue Agar CAS assay, following the
606 method described by Loudon et al. (2011). SA187 was spotted onto CAS plates and incubated at
607 28°C for 48 hours. The appearance of a clear zone around and beneath the spotted culture
608 indicated a positive result for siderophore production.

609 **Data availability**

610 The data set supporting the results of this article is included within the article and its additional
611 files. The raw data from the RNA-seq samples RNA-Seq data are available at NCBI's Gene
612 Expression Omnibus GEO Series accession number GSE251796
613 (<https://www.ncbi.nlm.nih.gov/geo/query/acc.cgi?acc=GSE251796>). The raw mass
614 spectrometry proteomics data have been deposited to the ProteomeXchange Consortium via the
615 PRIDE partner repository with the dataset identifier PXD047231.

616 **Funding**

617 This publication is based upon work supported by the King Abdullah University of Science and
618 Technology (KAUST), base fund for HH no. BAS/1/1062-01-01. JPR was supported by the
619 Agropolis Fondation (Flagship Project CalClim grant no. 1802-002).

620 Author contributions

621 KS and HH conceived and designed the study. KS standardized the high light stress protocol,
622 phenotyping experiments, and analyzed the data. AV performed bioinformatics analysis on the
623 raw RNA-seq data, while AP assisted in RNA-seq library preparation. NR carried out proteome
624 data analysis. AF, OA, and GXGR contributed to phenotyping experiments, and KF provided
625 support with confocal microscopy. SP submitted RNA-seq data and assisted with analysis. JPR
626 supervised the ro-GFP2 experiments. APN analyzed SA187 genome. HH supervised the
627 experiments and analysis of the data. KS and HH wrote the manuscript. HH, JPR and NR edited
628 the manuscript. All authors approved the final version of the manuscript.

629 Acknowledgements

630 We thank all members of the Hirt Lab, the CDA management and greenhouse facility team of
631 KAUST for the technical assistance.

632 Conflict of interest

633 The authors declare that they have no conflict of interest.

634

635

636

637

638

639

640

641

642

643

644

645

646

647

648

649

650

651

652

653

654 **Reference**

655

656 **Andrés-Barrao C, Lafi FF, Alam I, de Zélicourt A, Eida AA, Bokhari A, Alzubaidy H, Bajic VB, Hirt H, Saad**
657 **MM. 2017.** Complete genome sequence analysis of *Enterobacter* sp. SA187, a plant multi-stress
658 tolerance promoting endophytic bacterium. *Frontiers in Microbiology* **8**: 2023.

659

660 **Andrews S 2010.** FastQC: a quality control tool for high throughput sequence data: Babraham
661 Bioinformatics, Babraham Institute, Cambridge, United Kingdom.

662

663 **Apel K, Hirt H. 2004.** Reactive oxygen species: metabolism, oxidative stress, and signal transduction.
664 *Annu. Rev. Plant Biol.* **55**: 373-399.

665

666 **Arnon D. (1949).** Copper Enzymes in Isolated Chloroplasts. Polyphenoloxidase in *Beta Vulgaris*. *Plant*
667 *Physiology* **24**: 1- 15.

668

669

670 **Barczak-Brzyżek A, Brzyżek G, Koter M, Siedlecka E, Gawroński P, Filipecki M. 2022.** Plastid retrograde
671 regulation of miRNA expression in response to light stress. *BMC Plant Biology* **22**(1): 150.

672 **Bolger AM, Lohse M, Usadel B. 2014.** Trimmomatic: a flexible trimmer for Illumina sequence data.
673 *Bioinformatics* **30**(15): 2114-2120.

674

675 **Cheng N-H, Liu J-Z, Liu X, Wu Q, Thompson SM, Lin J, Chang J, Whitham SA, Park S, Cohen JD. 2011.**
676 *Arabidopsis* monothiol glutaredoxin, AtGRXS17, is critical for temperature-dependent
677 postembryonic growth and development via modulating auxin response. *Journal of Biological*
678 *Chemistry* **286**(23): 20398-20406.

679

680 **Cheng N, Yu H, Rao X, Park S, Connolly EL, Hirschi KD, Nakata PA. 2020.** Alteration of iron responsive
681 gene expression in *Arabidopsis* glutaredoxin S17 loss of function plants with or without iron
682 stress. *Plant signaling & behavior* **15**(6): 1758455.

683

684 **d'Alessandro S, Beaugelin I, Havaux M. 2020.** Tanned or sunburned: how excessive light triggers plant
685 cell death. *Molecular Plant* **13**(11): 1545-1555.

686

687 **de Zélicourt A, Synek L, Saad MM, Alzubaidy H, Jalal R, Xie Y, Andrés-Barrao C, Rolli E, Guerard F,**
688 **Mariappan KG. 2018.** Ethylene induced plant stress tolerance by *Enterobacter* sp. SA187 is
689 mediated by 2-keto-4-methylthiobutyric acid production. *PLoS genetics* **14**(3): e1007273.

690

691 **Dard A, Weiss A, Bariat L, Auverlot J, Fontaine V, Picault N, Pontvianne F, Riondet C, Reichheld J-P.**
692 **2023.** Glutathione-mediated thermomorphogenesis and heat stress responses in *Arabidopsis*
693 *thaliana*. *Journal of experimental botany* **74**(8): 2707-2725.

694

695 **Fryer MJ, Ball L, Oxborough K, Karpinski S, Mullineaux PM, Baker NR. 2003.** Control of Ascorbate
696 Peroxidase 2 expression by hydrogen peroxide and leaf water status during excess light stress
697 reveals a functional organisation of *Arabidopsis* leaves. *The Plant Journal* **33**(4): 691-705.

698

699 **Fricker MD. 2016.** Quantitative redox imaging software. *Antioxidants & redox signaling* **24**(13): 752-762.

700

- 701 **García-Quirós E, Alché JdD, Karpinska B, Foyer CH. 2020.** Glutathione redox state plays a key role in
702 flower development and pollen vigour. *Journal of experimental botany* **71**(2): 730-741.
703
- 704 **Gleason FK, Holmgren A. 1988.** Thioredoxin and related proteins in procaryotes. *FEMS microbiology*
705 *reviews* **4**(4): 271-297.
706
- 707 **Goss R, Lepetit B. 2015.** Biodiversity of NPQ. *Journal of plant physiology* **172**: 13-32.
708
709
- 710 **Grant CM. 2001.** Role of the glutathione/glutaredoxin and thioredoxin systems in yeast growth and
711 response to stress conditions. *Molecular microbiology* **39**(3): 533-541.
712
- 713 **Handara VA, Illya G, Tippabhotla SK, Shivakumar R, Budiman AS. 2016.** Center for Solar Photovoltaics
714 (CPV) at Surya University: novel and innovative solar photovoltaics system designs for tropical
715 and near-ocean regions (an overview and research directions). *Procedia Engineering* **139**: 22-31.
716
- 717 **Harbort CJ, Hashimoto M, Inoue H, Niu Y, Guan R, Rombolà AD, Kopriva S, Voges MJEEE, Sattely ES,**
718 **Garrido-Oter R, et al. 2020.** Root-Secreted Coumarins and the Microbiota Interact to Improve
719 Iron Nutrition in Arabidopsis. *Cell Host Microbe*: 825-837.e6. doi: 10.1016/j.chom.2020.09.006.
720
- 721 **Hendrix S, Dard A, Meyer AJ, Reichheld J-P. 2023.** Redox-mediated responses to high temperature in
722 plants. *Journal of experimental botany* **74**(8): 2489-2507.
723
- 724 **Holmgren A. 1989.** Thioredoxin and glutaredoxin systems. *Journal of Biological Chemistry* **264**(24):
725 13963-13966.
- 726 **Huang J, Zhao X, Chory J. 2019.** The Arabidopsis transcriptome responds specifically and dynamically to
727 high light stress. *Cell Reports* **29**(12): 4186-4199. e4183.
728
729
- 730 **Jung H-S, Crisp PA, Estavillo GM, Cole B, Hong F, Mockler TC, Pogson BJ, Chory J. 2013.** Subset of heat-
731 shock transcription factors required for the early response of Arabidopsis to excess light.
732 *Proceedings of the National Academy of Sciences* **110**(35): 14474-14479.
733
- 734 **Kapoor D, Sharma R, Handa N, Kaur H, Rattan A, Yadav P, Gautam V, Kaur R, Bhardwaj R. 2015.** Redox
735 homeostasis in plants under abiotic stress: role of electron carriers, energy metabolism
736 mediators and proteinaceous thiols. *Frontiers in Environmental Science* **3**: 13.
737
- 738 **Kasahara M, Kagawa T, Oikawa K, Suetsugu N, Miyao M, Wada M. 2002.** Chloroplast avoidance
739 movement reduces photodamage in plants. *Nature* **420**(6917): 829-832.
740
- 741 **Kim D, Perteza G, Trapnell C, Pimentel H, Kelley R, Salzberg SL. 2013.** TopHat2: accurate alignment of
742 transcriptomes in the presence of insertions, deletions and gene fusions. *Genome biology* **14**(4):
743 1-13.
744
745
- 746 **Kim G-T, Yano S, Kozuka T, Tsukaya H. 2005.** Photomorphogenesis of leaves: shade-avoidance and
747 differentiation of sun and shade leaves. *Photochemical & Photobiological Sciences* **4**: 770-774.
748

- 749
750 **Kleine T, Kindgren P, Benedict C, Hendrickson L, Strand A. 2007.** Genome-wide gene expression
751 analysis reveals a critical role for CRYPTOCHROME1 in the response of Arabidopsis to high
752 irradiance. *Plant physiology* **144**(3): 1391-1406.
753
- 754 **Knuesting J, Riondet C, Maria C, Kruse I, Bécuwe N, König N, Berndt C, Tourrette S, Guillemint-**
755 **Montoya J, Herrero E. 2015.** Arabidopsis glutaredoxin S17 and its partner, the nuclear factor Y
756 subunit C11/negative cofactor 2 α , contribute to maintenance of the shoot apical meristem
757 under long-day photoperiod. *Plant physiology* **167**(4): 1643-1658.
758
- 759 **Kumar A, Kumar V, Dubey AK, Ansari MA, Narayan S, Meenakshi, Kumar S, Pandey V, Pande V, Sanyal**
760 **I. 2021.** Chickpea glutaredoxin (CaGrx) gene mitigates drought and salinity stress by modulating
761 the physiological performance and antioxidant defense mechanisms. *Physiology and Molecular*
762 *Biology of Plants* **27**(5): 923-944.
763
- 764 **Louden B C., Haarmann D, Lynne, A. 2011.** Use of blue agar CAS assay for siderophore detection. *J.*
765 *Microbiol. Biol. Educ.* **12**: 51–53. doi: 10.1128/jmbe.v12i1.249
766
- 767 **Lucena C, Romera FJ, García MJ, Alcántara E, Pérez-Vicente R. 2015.** Ethylene participates in the
768 regulation of Fe deficiency responses in Strategy I plants and in rice. *Frontiers in Plant Science* **6**:
769 1056.
770
- 771
772 **Lu T, Meng Z, Zhang G, Qi M, Sun Z, Liu Y, Li T. 2017.** Sub-high temperature and high light intensity
773 induced irreversible inhibition on photosynthesis system of tomato plant (*Solanum lycopersicum*
774 L.). *Frontiers in Plant Science* **8**: 365.
775
- 776 **Martins L, Knuesting J, Bariat L, Dard A, Freibert SA, Marchand CH, Young D, Dung NHT, Voth W,**
777 **Debures A. 2020.** Redox modification of the iron-sulfur glutaredoxin GRXS17 activates holdase
778 activity and protects plants from heat stress. *Plant physiology* **184**(2): 676-692.
779
- 780 **Melicher P, Dvořák P, Krasylenko Y, Shapiguzov A, Kangasjärvi J, Šamaj J, Takáč T. 2022.** Arabidopsis
781 iron superoxide dismutase FSD1 protects against methyl viologen-induced oxidative stress in a
782 copper-dependent manner. *Frontiers in Plant Science* **13**: 823561.
783
- 784 **Mignolet-Spruyt L, Xu E, Idänheimo N, Hoeberichts FA, Mühlenbock P, Brosché M, Van Breusegem F,**
785 **Kangasjärvi J. 2016.** Spreading the news: subcellular and organellar reactive oxygen species
786 production and signalling. *Journal of experimental botany* **67**(13): 3831-3844.
787
- 788 **Montejano-Ramírez V, Valencia-Cantero E. 2023.** Cross-Talk between Iron Deficiency Response and
789 Defense Establishment in Plants. *Int J Mol Sci.* **24**(7):6236. doi: 10.3390/ijms24076236.
790
- 791 **Oliveros J 2016.** Venny. An interactive tool for comparing lists with Venn's diagrams. 2007–2015: cited
792 2021-07-15.
793
- 794 **Rey P, Becuwe N, Tourrette S, Rouhier N. 2017.** Involvement of Arabidopsis glutaredoxin S14 in the
795 maintenance of chlorophyll content. *Plant, Cell & Environment* **40**(10): 2319-2332.
796

- 797 **Rossel JB, Wilson IW, Pogson BJ. 2002.** Global changes in gene expression in response to high light in
798 *Arabidopsis*. *Plant physiology* **130**(3): 1109-1120.
799
- 800 **Rouhier N, Couturier J, Johnson MK, Jacquot J-P. 2010.** Glutaredoxins: roles in iron homeostasis. *Trends*
801 *in biochemical sciences* **35**(1): 43-52.
802
- 803 **Ruban AV. 2016.** Nonphotochemical chlorophyll fluorescence quenching: mechanism and effectiveness
804 in protecting plants from photodamage. *Plant physiology* **170**(4): 1903-1916.
805
- 806 **Schöttler MA, Tóth SZ. 2014.** Photosynthetic complex stoichiometry dynamics in higher plants:
807 environmental acclimation and photosynthetic flux control. *Frontiers in Plant Science* **5**: 188.
808
- 809 **Schumann T, Paul S, Melzer M, Dörmann P, Jahns P. 2017.** Plant growth under natural light conditions
810 provides highly flexible short-term acclimation properties toward high light stress. *Frontiers in*
811 *Plant Science* **8**: 681.
812
- 813 **Sedlak J, Lindsay RH. 1968.** Estimation of total, protein-bound, and nonprotein sulfhydryl groups in
814 tissue with Ellman's reagent. *Analytical biochemistry* **25**: 192-205.
815
- 816 **Shekhawat K, Saad MM, Sheikh A, Mariappan K, Al-Mahmoudi H, Abdulhakim F, Eida AA, Jalal R,**
817 **Masmoudi K, Hirt H. 2021.** Root endophyte induced plant thermotolerance by constitutive
818 chromatin modification at heat stress memory gene loci. *EMBO reports* **22**(3): e51049.
819
- 820
- 821 **Shi Y, Ke X, Yang X, Liu Y, Hou X. 2022.** Plants response to light stress. *Journal of Genetics and Genomics*.
822
- 823 **Sims DA, Gamon JA. 2002.** Relationships between leaf pigment content and spectral reflectance across a
824 wide range of species, leaf structures and developmental stages. *Remote Sensing of*
825 *Environment* **81**: 337 - 354.
826
- 827 **Sundaram S, Rathinasabapathi B. 2010.** Transgenic expression of fern *Pteris vittata* glutaredoxin PvGrx5
828 in *Arabidopsis thaliana* increases plant tolerance to high temperature stress and reduces
829 oxidative damage to proteins. *Planta* **231**: 361-369.
830
- 831 **Tian T, Liu Y, Yan H, You Q, Yi X, Du Z, Xu W, Su Z. 2017.** agriGO v2. 0: a GO analysis toolkit for the
832 agricultural community, 2017 update. *Nucleic acids research* **45**(W1): W122-W129.
833
- 834 **Trapnell C, Pachter L, Salzberg SL. 2009.** TopHat: discovering splice junctions with RNA-Seq.
835 *Bioinformatics* **25**(9): 1105-1111.
836
- 837 **Trapnell C, Roberts A, Goff L, Pertea G, Kim D, Kelley DR, Pimentel H, Salzberg SL, Rinn JL, Pachter L.**
838 **2012.** Differential gene and transcript expression analysis of RNA-seq experiments with TopHat
839 and Cufflinks. *Nature protocols* **7**(3): 562-578.
840
- 841 **Verbon EH, Trapet PL, Stringlis IA, Kruijs S, Bakker PAHM, Pieterse CMJ. 2017.** Iron and Immunity.
842 *Annual Review of Phytopathology* **55**: 355-375. [https://doi.org/10.1146/annurev-phyto-080516-](https://doi.org/10.1146/annurev-phyto-080516-035537)
843 [035537](https://doi.org/10.1146/annurev-phyto-080516-035537)
844

- 845 **Wada M. 2013.** Chloroplast movement. *Plant Science* **210**: 177-182.
846
847
- 848 **Walters RG. 2005.** Towards an understanding of photosynthetic acclimation. *Journal of experimental*
849 *botany* **56**(411): 435-447.
850
- 851 **Wiśniewski JR, Zougman A, Nagaraj N, Mann M. 2009.** Universal sample preparation method for
852 proteome analysis. *Nature methods* **6**(5): 359-362.
- 853 **Wu Q, Lin J, Liu JZ, Wang X, Lim W, Oh M, Park J, Rajashekar C, Whitham SA, Cheng NH. 2012.** Ectopic
854 expression of Arabidopsis glutaredoxin AtGRXS17 enhances thermotolerance in tomato. *Plant*
855 *Biotechnology Journal* **10**(8): 945-955.
856
857
- 858 **Yang C-L, Huang Y-T, Schmidt W, Klein P, Chan M-T, Pan I. 2022.** Ethylene response Factor109 attunes
859 immunity, photosynthesis, and iron homeostasis in arabidopsis leaves. *Frontiers in Plant Science*
860 **13**: 492.
- 861 **Yu H, Yang J, Shi Y, Donelson J, Thompson SM, Sprague S, Roshan T, Wang D-L, Liu J, Park S. 2017.**
862 Arabidopsis glutaredoxin S17 contributes to vegetative growth, mineral accumulation, and
863 redox balance during iron deficiency. *Frontiers in Plant Science* **8**: 1045.
- 864 **Zamioudis C, Hanson J, Pieterse, CM. 2014.** β -Glucosidase BGLU42 is a MYB72-dependent key regulator
865 of rhizobacteria-induced systemic resistance and modulates iron deficiency responses in
866 Arabidopsis roots. *The New phytologist*, 204(2), 368-379. <https://doi.org/10.1111/nph.12980>
- 867 **Zhang H, Liu P, Guo T, Zhao H, Bensaddek D, Aebersold R, Xiong L. 2019.** Arabidopsis proteome and the
868 mass spectral assay library. *Scientific data* **6**(1): 278.
869
870
871
872
873
874
875
876
877
878
879
880
881
882
883
884
885

886
887
888
889
890
891
892
893
894
895
896
897
898
899
900
901

902 **Figure 1. SA187 Induces High Light Stress Tolerance in *A. thaliana* and maintains Chlorophyll A**
903 **and B levels**

904 (A) Experimental Setup: *A. thaliana* seedlings were germinated for 5-days, with or without SA187. At day 6 colonized and non-
905 colonized seedlings were transferred to fresh 1/2MS and plates were exposed to Normal Light (NL) intensity of $130 \mu\text{mol m}^{-2} \text{s}^{-1}$
906 or High Light (HL) intensity of $1050 \mu\text{mol m}^{-2} \text{s}^{-1}$ and vertically grown for 10 d. (B) Phenotypic assessment of the beneficial effect
907 on the growth of 16-days old *A. thaliana* seedlings under NL (NL, NL+187) and HL (HL, HL+187) stress condition. (C) Fresh weight
908 of 16-day-old plants with and without SA187 under NL and HL regimes. (D-E) Chlorophyll A and Chlorophyll B in SA187 colonized
909 and non-colonized plants under NL control and HL stress conditions. All plots represent the means of 3 biological replicates. Error
910 bars indicate SD. Asterisks indicate a statistical difference based on Student's t-test * $P \leq 0.05$; ** $P \leq 0.01$; *** $P \leq 0.001$ for
911 differences between HL in comparison to HL+187 treatments. Scale bars correspond to 1 cm.

912
913

914 **Figure 2. Dynamic Transcriptome Responses of *A. thaliana* seedlings to Short-, Middle-, and Long-**
915 **Term High Light Stress**

916 Hierarchical clustering of up- and down-regulated DEGs in *A. thaliana* in response to 1h, 24h and 5d of Normal light (NL) and high
917 light (HL) exposure. For every gene, FPKM (Fragments Per Kilobase of transcript per Million mapped reads) values were
918 normalized. Red bars denote an increase, while green bars indicate a decrease in expression for a given gene. For the most
919 relevant clusters, gene families significantly enriched are indicated based on gene ontology. The pink line in each cluster indicates
920 an overall trend of differentially expressed genes in a particular cluster for different treatments. The 5-day-old seedlings were
921 transferred to new 1/2 MS plates before NL and HL treatments. The RNA-seq was performed with 1h, 24h and 5-days of HL-exposed
922 plants and their respective controls at NL condition. RNA-seq experiments were performed in three biological replicates.

923

924 **Figure 3. SA187 Reprograms the *A. thaliana* Transcriptome to Improve Photosynthesis and**
925 **Oxidative Stress after 24 h (A) and 5 days (B) of HL stress**

926 (A) Hierarchical clustering of up- and down-regulated DEGs in SA187 colonized and non-colonized *A. thaliana* seedlings in response
927 to 24h of normal light (NL) and high light (HL) exposure. (B) Hierarchical clustering of up- and down-regulated DEGs in SA187
928 colonized and non-colonized *A. thaliana* seedlings in response to 5 days of HL and NL exposure. Red bars denote an increase,

929 while green bars indicate a decrease in expression for a given gene. For the most relevant clusters, gene families significantly
 930 enriched are indicated based on gene ontology. 5-day-old seedlings +/- SA187 were transferred to new ½ MS plates before NL
 931 and HL treatments. The RNA-seq was performed with 24 h and 5-days of HL-exposed plants and their respective controls at NL
 932 condition with and without SA187. RNA-seq experiments were performed in three biological replicates.

933

934 Figure 4. SA187-Mediated Plant Growth Rescue under High Light Stress Involves Iron

935 (A) Phenotypic assessment of SA187 inoculation on growth of *A. thaliana* seedling grown on +Fe (sufficient iron, 18mg/L
 936 FeNaEDTA), Low iron (4mg/L FeNaEDTA,) and no iron (0mg/L FeNaEDTA) conditions. (B) Fresh weight of 16-day-old plants with
 937 and without SA187 grown under +Fe (sufficient iron), Low iron and no iron conditions stress conditions. (C-D) Phenotypic
 938 assessment (C) and fresh weight analysis of SA187 colonized, non-colonized Col-0 and indicated mutants *irt1-1* plants (reductive
 939 import of iron pathway) grown in NL and HL conditions for 10 days. (E) Fresh weight of 16-day-old SA187 colonized, non-colonized
 940 *A. thaliana* seedlings grown on +Fe (Sufficient iron, 18mg/L FeNaEDTA) and -Fe (Low iron, 8mg/L FeNaEDTA) 1/2MS-media plates
 941 under NL and HL regimes. (F) Fresh weight of Col-0 plants after doubling (36 mg/L FeNaEDTA) the Fe concentration (++Fe) under
 942 NL and HL regimes with and without SA187. (G) Shoot and root iron content of SA 187-colonized and colonized plants under
 943 normal light. (h) Shoot and root iron content of SA187-colonized and non-colonized plants under HL stress measured by ICP-MS.
 944 All plots represent the means of 3 biological replicates. Error bars indicate SD. Asterisks indicate a statistical difference based on
 945 Student's t-test *P ≤ 0.05; **P ≤ 0.01; ***P ≤ 0.001 for differences between HL in comparison to HL+187 treatments and HL++Fe
 946 (36 mg/L FeNaEDTA).

947

948 Figure 5. SA187 Reduces ROS levels to maintain plant Photosynthetic Performance in High Light 949 Stress

950 (A) Accumulation of superoxide radicals (visualized by nitroblue tetrazolium staining) in NL (normal light, control) and HL (high
 951 light stress) +/-SA187 plants. (B) In vivo monitoring of redox state upon high light stress. Cytosolic ro-GFP2 fluorescence from
 952 confocal images of plants treatment with DTT, H₂O₂ (top two images) and SA187 colonized and non-colonized plant leaf under 5
 953 days high light stress. Cytosolic ro-GFP2 fluorescence was collected at 505-530 nm after excitation with either 405 nm or 488 nm.
 954 (C) Ratio images were calculated as the 405/488 nm fluorescence from SA187 colonized and non-colonized plants exposed to HL
 955 stress for 0h, 24h, 5- and 10-days. (D) Ratio images were calculated as the 405/488 nm fluorescence from 10mM DTT and 100mM
 956 H₂O₂ exposed 10-days old plants. (E) Fresh weight of SA187-colonized or non-colonized wild-type Col-0 and *cad2-1* mutant plants
 957 upon long-term exposure to normal light and high light treatments. All plots represent the means of 3 biological replicates. Error
 958 bars indicate SE. Asterisks indicate a statistical difference based on Student's t-test *P ≤ 0.05; **P ≤ 0.01; ***P ≤ 0.001 for
 959 differences between HL in comparison to HL+187 treatments. Scale bars correspond to 1 cm.

960

961 Figure 6. Ethylene is a Main Regulator of SA187-Mediated High Light Stress Tolerance

962 (A) Fresh weight of SA187-colonized or non-colonized wild-type Col-0, and *ein3-1* mutant plants upon long-term exposure to
 963 normal light and high light. (B, C) Fresh weight and phenotypic assessment of SA187-colonized or non-colonized wild-type Col-0,
 964 and *ein3-1* mutant plants under low iron (4 mg/L FeNaEDTA) conditions. (D, E) Transcript levels of *FRO2* (ferric reduction oxidase
 965 2) and *LHCB* (light-harvesting Chl a/b-binding) in Col-0 and *ein3-1* mutant plants after 24h of normal light (NL, NL+187) and high
 966 light exposure (HL, HL+187). (F, G) Transcript levels of *FRO2* (ferric reduction oxidase 2) and *LHCB* (light-harvesting Chl a/b-
 967 binding) in Col-0 and *ein3-1* mutant plants after 5days of normal light (NL, NL+187) and high light exposure (HL, HL+187). For
 968 transcript level analysis, the data were normalized to tubulin as a reference gene. All plots represent the means of 3 biological
 969 replicates. Error bars indicate SE. Asterisks indicate a statistical difference based on Student's t-test *P ≤ 0.05; **P ≤ 0.01; ***P ≤
 970 0.001 for differences between HL in comparison to HL+187 treatments. Scale bars correspond to 1 cm.

971

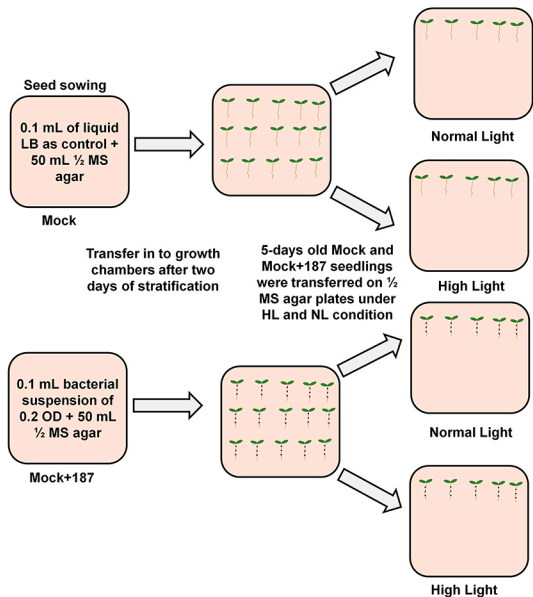
972 Figure 7. A model representing SA187-Mediated High Light stress Tolerance in *A. thaliana* 973 Through Ethylene-dependent Iron-assisted Redox Metabolism

974 The model illustrates the ethylene-dependent SA187-induced iron and sulfur metabolism in Arabidopsis. SA187-induced iron
 975 metabolism plays a crucial role in the biogenesis of Fe-S clusters and the maintenance of Fe-S cluster-containing proteins,
 976 essential for the electron transport chain (ETC). Additionally, SA187-induced sulfate is utilized for the formation of Fe-S clusters

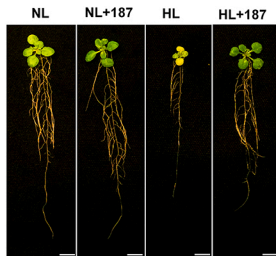
977 and can be converted into either glutathione (GSH). GSH, in turn, participates in reducing the oxidation of thiol-containing
978 proteins through the glutathione/glutaredoxin-dependent redox metabolism, ultimately mitigating high light-induced ROS.
979 HL= high light; PSII= photosystem II; Cytb= Cytochrome b; PSI= photosystem I; O₂= Oxygen; ROS= Reactive oxygen species; Protein
980 (SH)= thiol containing protein; Protein (S)₂= Disulfide protein; GRX(S)₂= Oxidized glutaredoxins; GRX(SH)₂= Reduced
981 glutaredoxins; GSH= reduced glutathione; GSSG= Oxidized glutaredoxins; NADP⁺= Oxidized nicotinamide adenine dinucleotide
982 phosphate; NADPH= Reduced nicotinamide adenine dinucleotide phosphate
983

Journal Pre-proof

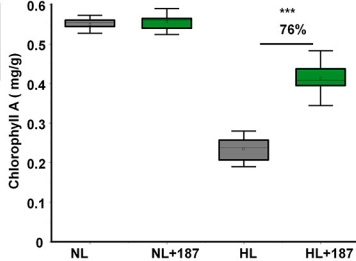
A



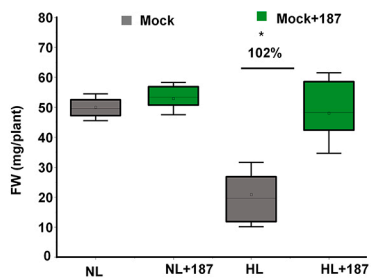
B



D



C



E

